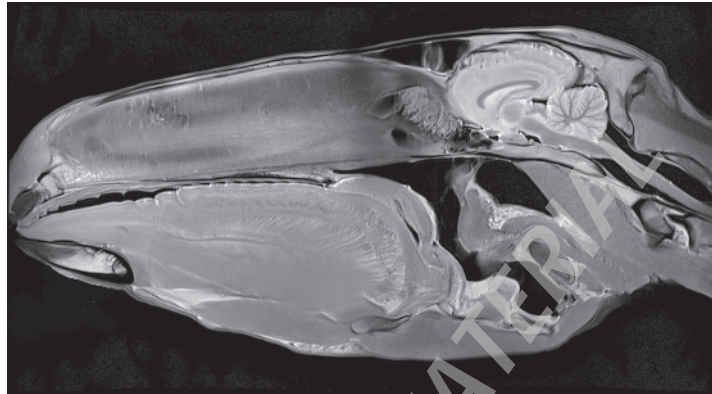# CHAPTER 1
Overview of CT and MRI of the Equine Head

The diagnosis of conditions affecting the equine head is challenging for the veterinary practitioner due to its large size, complex anatomy, and the multitude of different tissues present and thus the large number of potential disease processes. Disease processes of the teeth include caries, periodontal disease, tooth root abscess, tooth fracture, dentigerous cysts, and malocclusion to name a few [1]. The tongue can be affected by trauma, infection, or neoplasia. The nasal passages and paranasal sinuses are important parts of the equine head that can be the site of sinusitis, ethmoid hematomas, cysts, or neoplasia. The diverticulum of the auditory tube (guttural pouch) can develop fungal granulomas, empyema, blood clots, or tympany. Laryngeal hemiplegia, dorsal displacement of the soft palate, epiglottic entrapment, rostral displacement of the palatopharyngeal arches, arytenoid chondritis, and pharyngeal narrowing can affect the pharyngeal region [2]. Other tissues in the head such as the lymph nodes and salivary glands can be affected by infectious or non-infectious inflammation, or neoplasia. The brain can be affected by trauma, bleeding, infarction, neoplasms, cholesterinic granulomas, ventriculomegaly (hydrocephalus), and infection (meningitis or meningoencephalitis). Trauma to the head can result in fractures of the calvarium, mandible, temporomandibular joint, basisphenoid bone, and nuchal crest of the occipital bone. Although uncommon in horses, neoplasia that can be found in the head includes melanoma, adenocarcinoma or rhabdomyosarcoma of the tongue, lacrimal gland adenocarcinoma and ophthalmic tumors associated with the eye, and multicentric lymphoma affecting the lymph nodes in the head [2]. The hyoid bones can be affected by fractures or temporohyoid osteoarthropathy. The eyes and ears are also prone to a variety of pathological conditions. Many of these conditions can be diagnosed on physical examination; however, many require further diagnostics.

Diagnostic imaging of the equine head is most commonly done via radiography (Figure 1) or endoscopy. Routine radiographic examination can include orthogonal projections of the area of interest, oblique projections of the dental arcades or temporomandibular joints and intraoral projections for the rostral mandible/maxilla. Due to the size of the adult head and the limited size of the X-ray cassette or imaging plate, multiple radiographs are needed to image the entire head, although this is not routinely performed in clinical practice. Radiographs offer superior spatial resolution compared to more advanced imaging options; however, due to the superimposition of anatomy, lesion localization can be quite challenging using radiography. The anatomy of the head is complex and radiographs

(a)

(b)
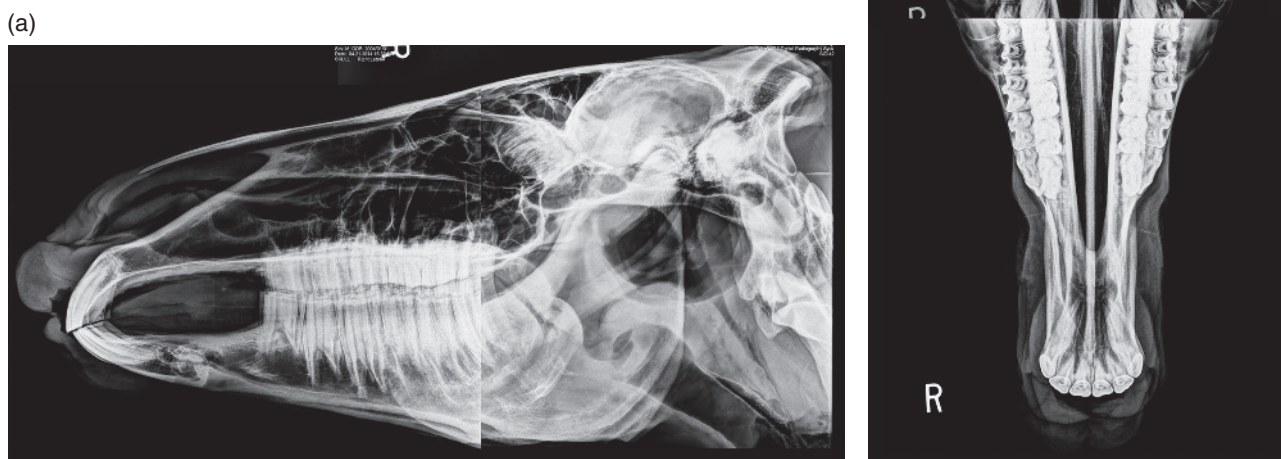
Figure 1 A lateral (a) and dorsoventral radiograph (b) of the head from an older adult equine cadaver that was used in the making of this book. Two radiographs are spliced together to create each image of the whole head. These radiographs demonstrate the excellent contrast between the air-filled nasal passages, paranasal sinuses and guttural pouches, and the mineral opaque bones and teeth. The soft tissues are difficult to differentiate unless they are surrounded by gas or bone.

do not provide adequate contrast of the soft tissues of the head. Radiographic anatomy has been thoroughly described elsewhere and is outside the scope of this book.

A computed tomography (CT) unit consists of a high-powered X-ray tube mounted in a circular gantry across from a detector array. The gantry is able to rotate around the patient using slip-ring technology so it is not tethered electronically to the rest of the unit. As the gantry rotates, the patient moves either into or out of the gantry as the X-rays are absorbed, scattered, or pass through the patient. The X-rays that reach the detector array are used to construct an image.

For digital radiographs, the attenuation of the X-rays results in a two-dimensional image involving multiple pixels. CT uses a similar method to display an image by converting a volume of tissue to a three-dimensional pixel called a voxel. CT will determine the average linear attenuation coefficient of X-rays for each voxel in a patient at a particular location [3]. Each voxel can be given a quantifiable number in terms of its gray scale, termed a Hounsfield unit (HU). As a reference, pure water has a HU of 0 and air is –1000 HU. Adipose tissue can vary from –30 to –80 HU, soft tissues +30 to +220, while bone and iodinated contrast media can be close to +2000 to +3000. Each voxel is then interpreted as a pixel when displayed as a two-dimensional CT image.

Most CT images are reconstructed in an axial plane. If the depth of the slice thickness (z-direction of the voxel) is the same as the size of the pixel (x and y directions), then the voxel is considered isotropic, or near isotropic if it is similar in size. Isotropic voxels allow for high-resolution reconstructions of the CT dataset into multiple different planes. These reconstructions allow one to view the anatomy in different planes to identify the extent of a disease process or to better visualize the "three-dimensional" (3D) anatomy using a two-dimensional interface. Isotropic voxels can also be used to produce high-resolution reconstructions that appear three-dimensional, even though they are still a two-dimensional image. This is demonstrated in Figure 2c and d, where a 3D reconstruction can be useful to get an overall look at the scanned anatomical structures.

Computed tomography images are reconstructed from a very large collection of voxels (raw image data), each with its own Hounsfield unit and location in space. The computer uses an algorithm or filter to adjust how each pixel looks on a two-dimensional image and this algorithm can be modified to alter the spatial resolution and contrast differences of different tissues. The primary two algorithms used in this book are referred to generically as a bone filter or algorithm and a soft tissue filter or algorithm. The bone algorithm has a higher spatial resolution and the bone and teeth are seen in gray with well-defined edges, whereas all the soft tissues are homogenously gray. The soft tissue algorithm has a reduced spatial resolution but the contrast of the soft tissues is more noticeable, and the bone and teeth are completely white.

The appearance of the CT images can be adjusted by the viewer for either algorithm using the window width/window level adjustment function found on all image viewing systems. The window width (WW) is the range of displayed Hounsfield units. The window level (WL) is the Hounsfield unit in the center of the window width. In this book, the bone algorithm is shown in a bone window, with a WW of ~3500 and a WL of ~650. The soft tissue algorithm is shown in a soft tissue window, with a WW of ~500 and a WL of ~70. So, for the bone setting a wide window of 3500 densities allows for a lot of different densities to be displayed, centered on 650 HU (+4150 to –2850 HU). For the soft tissue setting, a short window width of 500 is used, centered at 70 HU, near the density of the soft tissues of the head (+570 HU to –430 HU). Anything with a higher density than these ranges will be white, and anything with a lower density will be black. Everything in between will be a shade of gray. For viewing the brain, an even smaller window is needed to assess the difference between gray and white matter. These images were not used to depict the brain anatomy in this book due to space requirements. Figure 3 demonstrates the brain WW/WL in a horse with cholesterinic granulomas and ventriculomegaly.

Magnetic resonance imaging (MRI) is another cross-sectional imaging modality, but unlike CT, it does not involve ionizing radiation Instead, MRI uses nuclear magnetic resonance, the absorption and release of energy from the nucleus of an atom when placed in a strong magnetic field. Although different atoms can be used for imaging, in living tissue primarily hydrogen is used as it has the largest magnetic moment and is in greatest abundance in water and fat [3]. The nucleus of the hydrogen atom, which consists of a proton, is the focus for generating the MR signal. The patient is placed on the MRI table with the body part of interest to be imaged within a coil. This coil allows radiofrequency signals to be emitted, received, or both. This radiofrequency energy is absorbed by the protons in the body and emitted at certain rates (T2 and T1 relaxation). There are multiple different types of MR sequences that can be performed, and for the most part they are related to timing differences of the emitted energy from the protons, or relaxation times. These sequences include T2 weighted, T1 weighted, T2* weighted, proton density (PD), and inversion recovery (fat or fluid suppression).

T2-weighted sequences are primarily used to identify pathology such as inflammation or edema. The T2 relaxation between different tissues allows for the excellent contrast seen between cerebrospinal fluid (CSF), gray and white matter of the brain, and fat (Figure 4a,d). With T1-weighted sequences, the contrast between the CSF, gray and white matter, and the fat is reduced, but the resolution and anatomic detail are improved. Also, contrast media (gadolinium based) can be administered intravenously and assessed with T1-weighted imaging (Figure 4c) to increase lesion conspicuousness. This contrast medium reduces the T1 relaxation time, resulting in increased signal intensity on T1-weighted sequences [4]. This increased signal is present within blood vessels and in tissues that have an increased blood flow. In brain tissue, this would result from a break down of the blood–brain barrier.

Proton density contrast weighting depends on the difference in magnetized protons within different tissues [3]. This sequence results in proton-dense tissues such as CSF having a high (bright) signal intensity. This leads to the highest overall
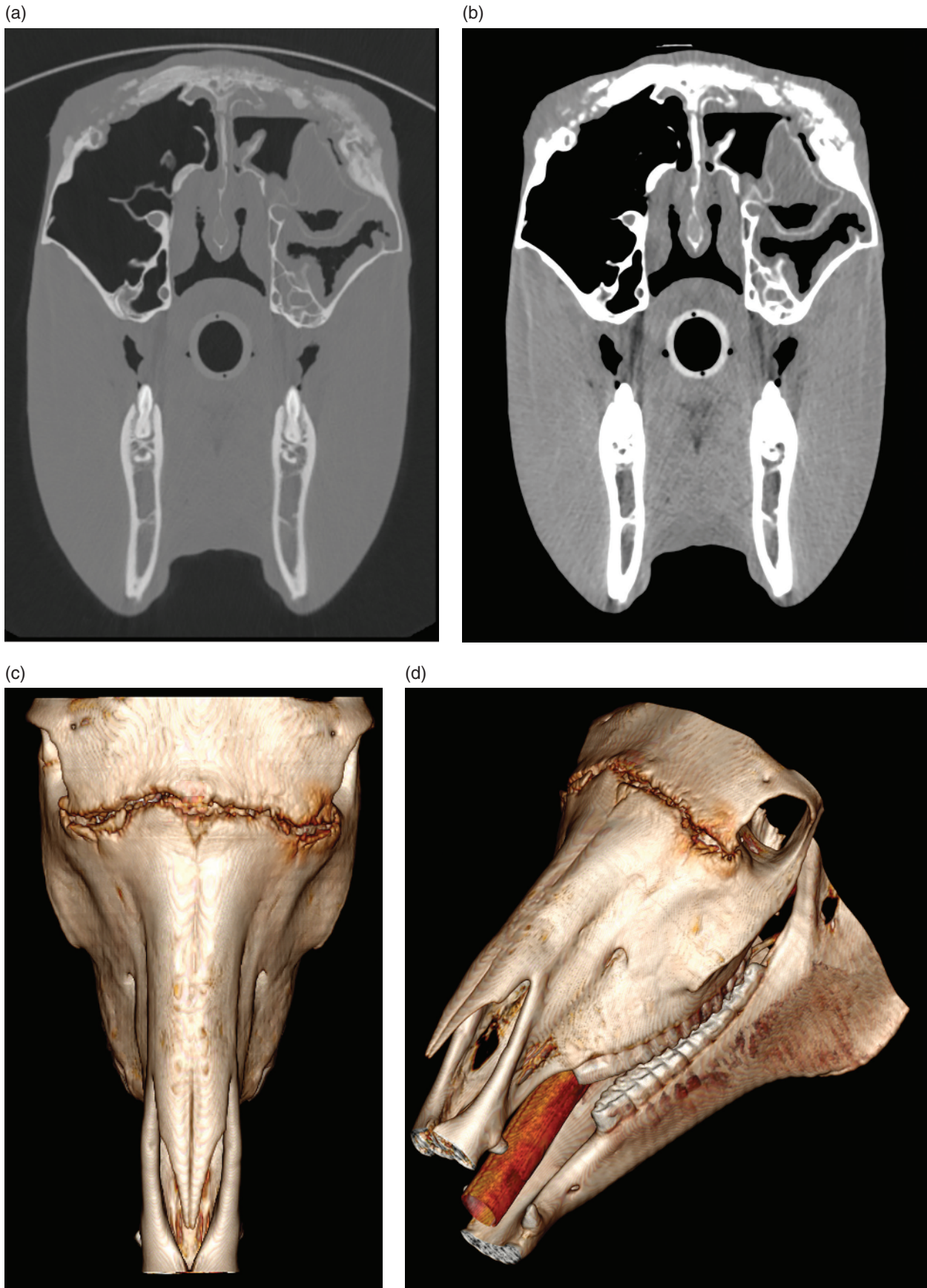
Figure 2 CT scan of an adult horse that presented with a facial deformity from an unknown trauma and signs of sinusitis. The patient was imaged in dorsal recumbency for the CT scan. (a,b) Transverse images at the level of the fracture in a bone filter and window (a) and a soft tissue filter and window (b), demonstrating thickened and irregular margins of the frontal, nasal, and lacrimal bones. Fluid is also noted in the conchofrontal sinus and caudally displaced ventral conchal sinus. The lining of the sinuses is thickened, consistent with sinusitis. (c,d) "Three-dimensional" reconstructions of the CT dataset with a dorsal view (c) and left dorsolateral view (d) of the skull. These images help to get an overall look at the bones of the skull and to determine that this deformity was likely caused by a concussive trauma to a sharp linear object, such as the corner of a beam or post. The displacement of the ventral conchal sinus and concha caused by the trauma caused narrowing of the conchomaxillary opening that impeded drainage, resulting in the sinusitis.
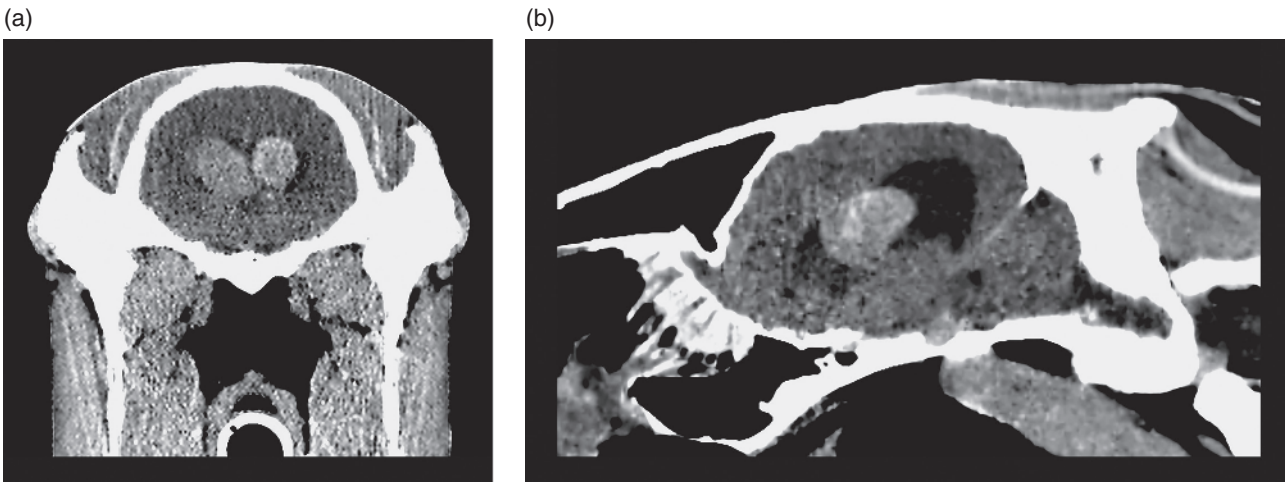
Figure 3 Transverse (a) and sagittal (b) reconstructions of a CT scan of an adult horse that presented with a history of seizures. The WW is 83 and WL is 27. Within each lateral ventricle is an ovoid, faintly mineral-dense structure arising from the choroid plexus. There is also fluid distension of the lateral ventricles, consistent with an obstruction to CSF outflow. These mineralized structures are consistent with cholesterinic granulomas causing an obstructive hydrocephalus.
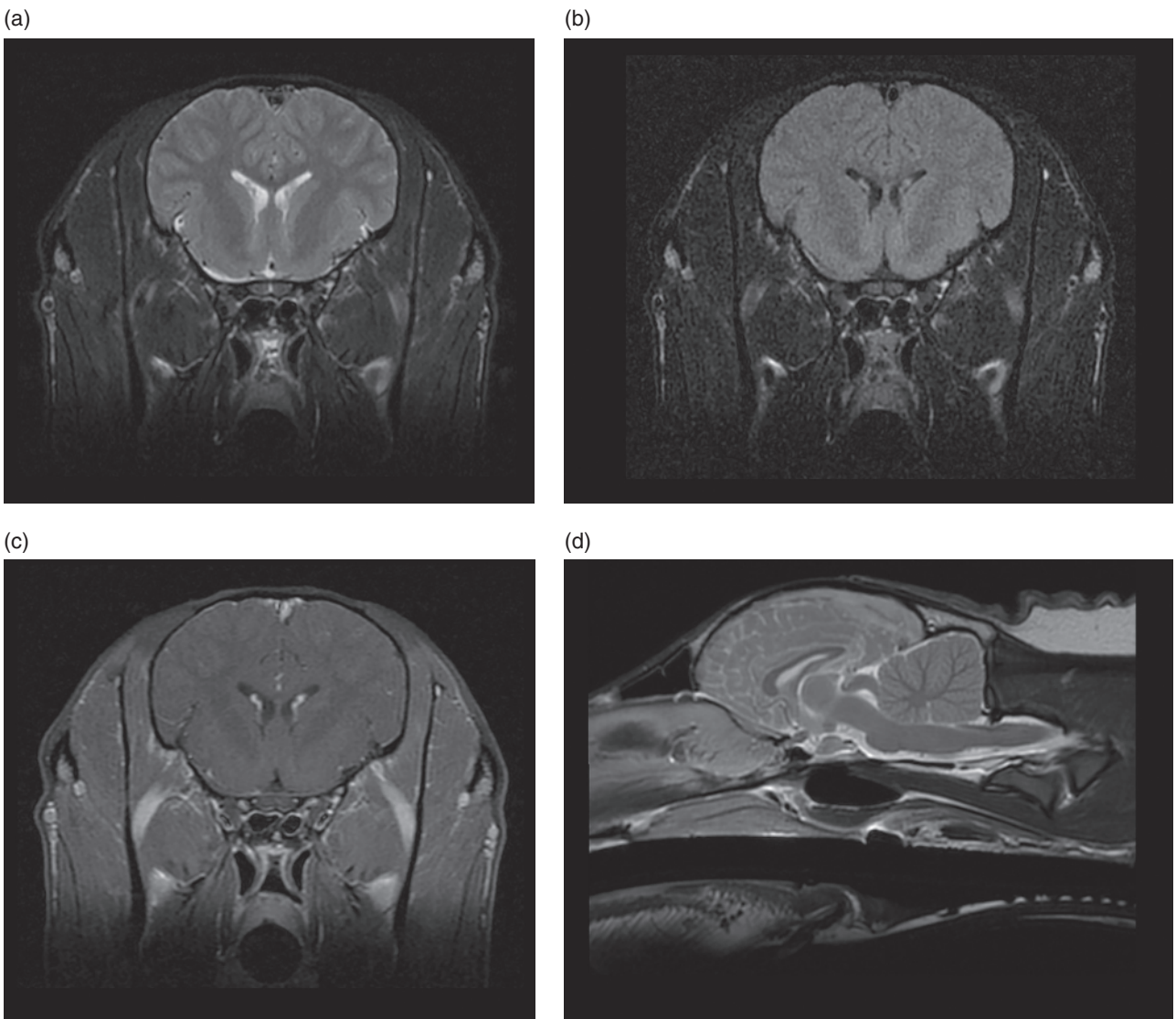
Figure 4 MRI images of a young horse. (a–c) Transverse MR images of the rostral third of the cerebrum at the level of the lateral ventricles. (a) T2-weighted sequence. (b) FLAIR sequence. (c) T1-weighted sequence plus contrast administration (gadolinium) and fat saturation. Note the fluid suppression of the CSF on the FLAIR sequence (b) in the lateral ventricles when compared to (a). (d) Sagittal plane, T2-weighted sequence of the brain on midline. In (c), there is contrast enhancement of the choroid plexus in the lateral ventricles, and the blood vessels ventral to the brain.

(a)

(b)

(c)
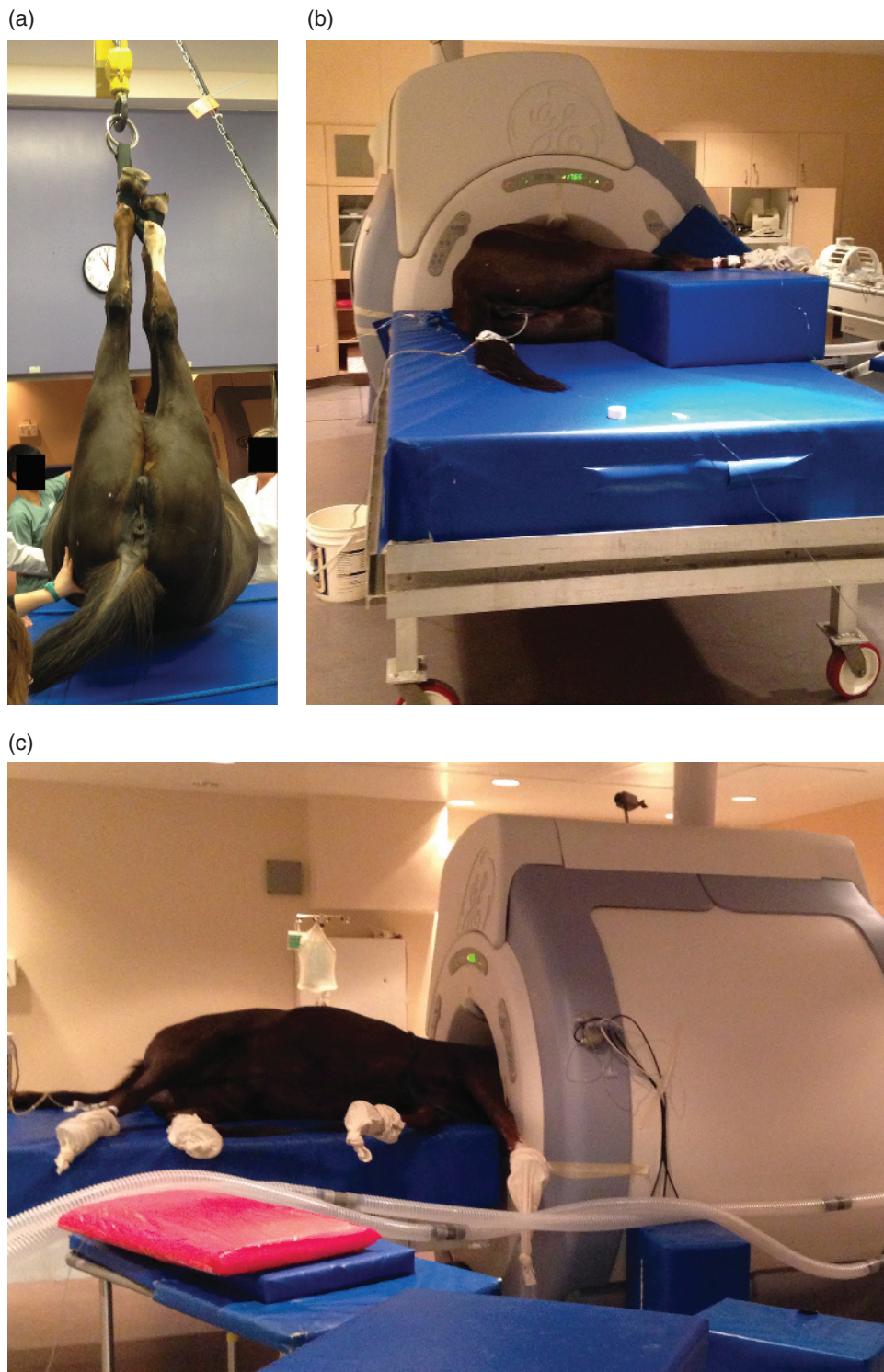
Figure 5 (a) An adult horse is raised onto the MRI table with hobbles placed around the feet and a ceiling hoist. The table is then rolled into the MRI suite, the wheels locked, and the patient moved forward into the magnet by sliding it across the padded table (b,c). (b) View from the MRI control room of the horse in the magnet. (c) Side view from the entry door of the horse in the magnet.

signal intensity and signal-to-noise ratio, while the image contrast is slightly reduced [3]. Inversion recovery is another type of MR sequence, and can null the signal from either fluid (fluid attenuation inversion recovery or FLAIR) or fat (short-tau inversion recovery or STIR). The FLAIR sequence is useful to differentiate pure fluid from proteinaceous fluid, and to better define the margins of a fluid-filled space or pocket. The STIR sequence is useful to identify pathology (inflammation, edema) without mistaking it for hyperintense fat. The last common type of sequence is a T2*-weighted sequence. This is susceptible to magnetic field inhomogeneities, and is particularly useful to identify hemoglobin breakdown products. A

(a)

(b)

(c)

(d)

Figure 6 An adult horse has been hoisted onto the large animal CT table and positioned in dorsal recumbency. (a) Back view of the horse. (b) Back and side view of the horse. (c) Side view of the horse. (d) Front view of the scanner with the horse intubated and connected to the anesthetic equipment.

more in-depth discussion of the physics of MRI and these sequences is beyond the scope of this book and can be learned elsewhere [3].

The proton density sequence images were chosen for this book based on the esthetics of the images when compared to T1- and T2-weighted images, the image contrast of the brain, and the adequate depiction of all the different anatomical structures in the head.

Equine CT and MRI scans require proper facilities and equipment for holding and moving the animals. At our facility, we have two different large animal tables. The table for MRI is non-ferromagnetic so it can be used in the MRI suite (Figure 5). A ceiling hoist is needed to move the patient from the induction stall to the table with the use of hobbles (Figure 5a). Large soft pads are needed under the patient to prevent muscle damage. The patient is moved so the area of interest (rostral or caudal portion of the head) is placed in the middle of the magnet (iso-center) (Figure 5b,c). The MRI large animal table does not move during scanning.

The large animal CT table is different from the MRI table as it connects directly to the smaller CT bed underneath, allowing the table to move during scanning. Patients are often imaged in dorsal recumbency, with the area of interest (rostral or caudal head) in the CT gantry (Figure 6). As the scan starts, the patient is moved out of the scanner until the region of interest is scanned. Intravenous iodinated contrast medium can be administered and the scan repeated.

Indications for performing CT versus MRI

At our institution, equine head CT scans are more frequently performed than MRI scans. These are typically used to evaluate the teeth and sinuses, and for fractures following trauma. CT allows for excellent visualization of the tooth roots, clear delineation of the nasal passages and paranasal sinuses, and partial visualization of the brain and soft tissues. MRI provides much better contrast of the brain and soft tissues of the head. A major limitation to doing an MRI of the brain of a horse is that the patient likely has neurological signs. This would also apply to neurological patients presenting for a CT scan of the head. Recovery of a neurological horse can be problematic and result

in head trauma or fractured limbs. MRI has been reported to be more sensitive to physiological processes of the head and central nervous system than CT, and has been successfully used as a neurodiagnostic modality in horses [5].

Both CT and MRI require general anesthesia and are expensive, with a limited number of institutions having the ability to image large animals with CT and/or MRI. The risk of the patient undergoing general anesthesia for a CT or MRI needs to be less than the potential benefit of the information gained from such a scan. For those patients that do undergo a cross-sectional imaging scan at your facility, this book should serve as a quick and useful reference to help you better understand the complex anatomy of the equine head.

Notes

The dorsal and sagittal MRI images have been stitched together using Siemens Composer software. This is not used for diagnostic purposes, but does give a better perspective of the anatomy in relation to the whole head and is very useful for the purposes of this book.

The sequence parameters for the PD MRI sequences were: TE 28, TR 6174.8, FS 3, 4.4 mm slice thickness. CT and MRI scans of the equine cadaver heads were performed by Animal Imaging, Irving, Texas.

References

1 O'Brien RT, Biller DS (1998) Dental imaging. *Veterinary Clinics of North America Equine Practitioner*, **14**, 259.

2 Reed SM, Bayly WM, Sellon DC (2010) *Equine Internal Medicine*, 3rd edn. Saunders Elsevier, St Louis.

3 Bushberg JT, Seibert JA, Leidholdt EM, Boone JM (2012) *The Essential Physics of Medical Imaging*, 3rd edn. Lippincott Williams and Wilkins, Philadelphia.

4 Saveraid TC, Judy CE (2012) Use of intravenous gadolinium contrast in equine magnetic resonance imaging. *Veterinary Clinics of North America, Equine Practitioner*, **28**, 617–636.

5 Ferrell EA, Gavin PR, Tucker RL, Sellon DC, Hines MT (2002) Magnetic resonance for evaluation of neurologic disease in 12 horses. *Veterinary Radiology and Ultrasound*, **43** (6), 510–516.